Properties of amphiphilic oligonucleotide films at the air/water interface and after film transfer

Keller, R.; Kwak, M.; de Vries, J. W.; Sawaryn, C.; Wang, J.; Anaya, M.; Muellen, K.; Butt, H. -J.; Herrmann, A.; Berger, R.

Published in:
Colloids and Surfaces B: Biointerfaces

DOI:
10.1016/j.colsurfb.2013.06.022

Publication date:
2013

Colloids and Surfaces B: Biointerfaces 111 (2013) 439–445

Contents lists available at SciVerse ScienceDirect

Colloids and Surfaces B: Biointerfaces

journal homepage: www.elsevier.com/locate/colsurfb

Properties of amphiphilic oligonucleotide films at the air/water interface and after film transfer

R. Keller[a], M. Kwak[b], J.W. de Vries[b], C. Sawaryn[a], J. Wang[a], M. Anaya[a], K. Müllen[a], H.-J. Butt[a], A. Herrmann[b], R. Berger[a,*]

[a] Max Planck Institute for Polymer Research, 55128 Mainz, Germany
[b] Department of Polymer Chemistry, Zernike Institute for Advanced Materials, University of Groningen, Nijenborgh 4, 9747 AG Groningen, The Netherlands

ARTICLE INFO

Article history:
Received 3 April 2012
Received in revised form 11 June 2013
Accepted 12 June 2013
Available online xxx

Keywords:
Scanning force microscopy
DNA block copolymers
Langmuir Blodgett films
Atomic force microscopy

ABSTRACT

The self-assembly of amphiphilic hybrid materials containing an oligonucleotide sequence at the air/water interface was investigated by means of pressure–molecular area (Π–A) isotherms. In addition, films were transferred onto solid substrates and imaged using scanning force microscopy. We used oligonucleotide molecules with lipid tails, which consisted of a single stranded oligonucleotide 11mer containing two hydrophobically modified 5-(dodec-1-ynyl)uracil nucleobases (dU11) at the 5′-end of the oligonucleotide sequence. The air/water interface was used as confinement for the self-assembling process of dU11. Scanning force microscopy of films transferred via Langmuir–Blodgett technique revealed mono-, bi- ($\Pi \geq 2$ mN/m) and multilayer formation ($\Pi \geq 30$ mN/m). The first layer was 1.6 ± 0.1 nm thick. It was oriented with the hydrophilic oligonucleotide moiety facing the hydrophilic substrate while the hydrophobic alkyl chains faced air. In the second layer the oligonucleotide moiety was found to face the air. The second layer was found to cover up to 95% of the sample area. Our measurements indicated that the rearrangement of the molecules into bi- and multiple bilayers happened already at the air/water interface. Similar results were obtained with a second type of oligonucleotide amphiphile, an oligonucleotide block copolymer, which was composed of an oligonucleotide 11mer covalently attached at the terminus to polypropyleneoxide (PPO).

1. Introduction

Oligonucleotide (ODN) molecules consisting of deoxyribonucleic acid monomers are particularly promising candidates for the design of new materials and macromolecular assemblies [1]. The highly specific binding through Watson–Crick base-pairing of oligonucleotides facilitates convenient creation of defined assemblies by molecular recognition. One strategy is to induce defined conformational changes by DNA hybridization to realize complex molecular machines in liquids [2,3]. A popular example is the design of molecular tweezers, which can be actuated by DNA hybridization, as reported by Yurke et al. [4]. One class of such oligonucleotide hybrid materials are amphiphilic molecules like oligonucleotide block copolymers [5,6] and oligonucleotides modified with small hydrophobic moieties [7,8]. The partial hydrophobicity of the oligonucleotide hybrid materials induces microphase separation in aqueous solution leading to the formation of self-assembled aggregates like micelles and lipid vesicles [5,9,10]. The micelle shape is tuneable by hybridization with tailored complementary oligonucleotide sequences [11]. Furthermore, such oligonucleotide amphiphiles were introduced into vesicles composed of phospholipids. In this regard, the surface of lipid vesicles could be easily functionalized by hybridization [12]. More sophisticated functions mediated by the DNA motif and specific base pairing of complementary sequences were vesicle aggregation and fusion [13–16]. In a similar manner oligonucleotides with lipid tails were doped in supported phospholipid bilayers allowing selective tethering of liposomes, enzymes, drugs or fluorescent probes and therewith fabricating highly functional surfaces [17]. Moreover, the use of hydrophobic moieties allows the organization of oligonucleotides at the air/water interface. Langmuir monolayers composed of single nucleosides functionalized with a lipid moiety have been investigated [18–20]. Recently, Caseli et al., have reported the use of diblock copolymers containing a poly(butadiene) block adsorbing to the air/water interface with the intention to study the interaction with cell membranes [21].

The molecule, which we have investigated in this regard is an amphiphilic oligonucleotide molecule (dU11) [22], which consists of a single stranded oligonucleotide (ssODN) 11mer containing two hydrophobically modified 5-(dodec-1-ynyl)uracil nucleobases at the terminal 5′-end of the oligonucleotide sequence (Fig. 1). Hereby, the alkyl chains of the dU11 act as arm floats for the oligonucleotide.

* Corresponding author.
E-mail address: berger@mpip-mainz.mpg.de (R. Berger).

0927-7765/$ – see front matter © 2013 Elsevier B.V. All rights reserved.
http://dx.doi.org/10.1016/j.colsurfb.2013.06.022

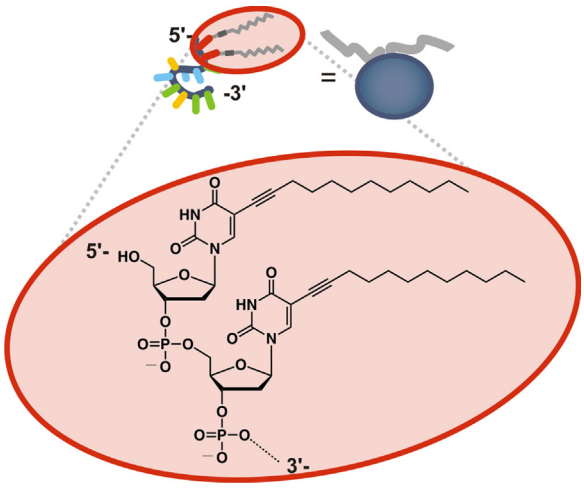

Fig. 1. Schematic diagram and chemical structure of the dU11. The oligonucleotide sequence is 5′-UUTGGCGTCTT-3′. U represents the hydrophobically modified 2′-deoxyribonucleotide containing 5-(dodec-1-ynyl)uracil. For sketches the structure is simplified by a blue oval (= ODN) and grey lines (= lipid tails).

The air/water interface was used as confinement for the aggregation of dU11 in order to prepare functional thin films in a subsequent transfer process onto a solid. However the alkyl chains are rather short and stable molecular monolayers at the air/water interface are not readily expected. Nevertheless we investigated the thin films after transfer onto a solid substrate with the aim to realize an orientation of the oligonucleotide moiety towards the air interface. Such an orientation would not be accessible in a classical Langmuir–Blodgett film scheme.

2. Materials and methods

2.1. Molecules

dU11 was synthesized and purified as reported previously by Anaya et al. [22]. Purity was controlled by $_{31}$P-NMR (100 MHz, THF-d 8) and MALDI-TOF MS as well as by ion exchange chromatography and polyacrylamide gel electrophoresis. For details see the Supporting Information as well as [22,23]. The self-assembly of these lipid-oligonucleotides in aqueous solution was investigated by light scattering experiments and revealed micelle sizes depending on the position and number of the hydrophobic moieties [22,24]. The critical micelle concentration (cmc), which is defined as concentration of an amphiphile above which micelles are formed, was determined to be cmc_{dU11} = 8.1 mg/L = 2.2 μmol/L [23]. The single stranded oligonucleotide 11mer sequence was designed to be non-self-complementary: 5′-UUTGGCGTCTT-3′ with 2 alkyl modified uracil bases at the 5′ end of the oligonucleotide sequence. Spreading solutions (c = 1.4 μmol/L) were prepared in dichloromethane (Chromasolv, Merck). As a second oligonucleotide amphiphile, the ODN-*b*-PPO molecule with one PPO block attached to the oligonucleotide was synthesized and purified as reported elsewhere [25]. The molecular weight of the PPO block was $M_{W,PPO}$ = 6800 g/mol. The single stranded oligonucleotide 11mer sequence was designed to be non-self-complementary: 5′-TTCTATAGAAA-3′ (the PPO block is attached to the 5′-end). Purity was determined via ion exchange chromatography and polyacrylamide gel electrophoresis. For details see Supporting Information and [22,23]. Spreading solutions (c = 0.25 μmol/L) were prepared in dichloromethane (Chromasolv, Merck). Water was purified to a resistance of 18.2 MΩ/cm using a Milli-Q filtration system (Millipore) and additionally distilled before use to ensure isotherm reproducibility.

The amphiphilic molecules were dissolved in Milli-Q water and the oligonucleotide concentration was determined by measuring a UV/vis absorption spectrum of the solution. The nominal concentration of the solutions for concentration determination was below the critical micelle concentration of dU11. The absorption at λ = 260 nm was used to determine the single stranded oligonucleotide concentration by applying Lambert Beers law. The respective molar extinction coefficient was calculated according to the oligonucleotide sequence (ε_{dU11} = 103 327 L/(mol cm); $\varepsilon_{ODN\text{-}b\text{-}PPO}$ = 128 667 L/(mol cm)).

2.2. Monolayer preparation

500 μL of the respective solution in dichloromethane were spread dropwise onto the distilled Milli-Q subphase with a microliter syringe. The cleanliness of the water subphase surface was verified by measurement of blind isotherms before spreading, which did not show any change in surface pressure. The spread layer was left for solvent evaporation for 15 min prior to each measurement. Isotherm measurements after 15 min and 85 min showed an identical isotherm course and confirmed that 15 min evaporation time are sufficient (Supporting Information Fig. S2).

2.3. Monolayer isotherms and monolayer transfer

Surface pressure versus molecular area (Π–A) isotherms were recorded on a Langmuir-Trough RK1 (Riegler und Kirstein GmbH, Potsdam Germany) with a total volume of 120 mL, which was equipped with a subphase exchanging system. A peristaltic pump was attached to the trough to remove the subphase (Minipuls 3, Abimed, Gilson Inc., United States). The surface pressure $\Pi = \gamma_0 - \gamma$, was measured using a Wilhelmy plate (filter paper); here, γ_0 is the surface tension of the pure subphase and γ is the surface tension at a certain amount of dU11. The subphase and room temperature were regulated to 20 °C. The temperature of the trough was controlled by a thermostat which was set to 20 °C. The tubings of the thermostat proceed in sinuous lines underneath the trough. Surface pressure was calibrated using arachidic acid as a reference. Isotherms were recorded at a high compression speed of 6.7 cm/min = 1090 Å^2 mol^{-1} min. Compression–expansion cycles were recorded leaving the monolayer to equilibrate for 15 min before recompression. For the isotherms shown in Fig. 2, the barriers were moved together to compress the film until the meniscus of the subphase moved over the rim, which caused a slope change in the isotherm. After expansion of the film, the subphase level was lowered by use of the subphase exchange system in order to reduce the measurement artifact caused by the meniscus shift. The slope change could not be found in the second compression cycle. In the third compression cycle, the final pressure was increased until a shift of the meniscus along the trough rim was observed again. Accordingly, the slope changes at high surface pressures (Π > 20 mN/m) are caused by this measurement artifacts and were thus not considered in the discussion.

Monolayers were transferred onto silicon wafers (both sides polished) by Langmuir–Blodgett (LB) film transfer [26]. The silicon wafers were treated in an Ar-Plasma (Plasma Cleaner/Sterilizer PDC-002, 200W, Harrick Scientific Corp., United States) for 10 min. They were stored and transported in Milli-Q water. For Langmuir–Blodgett (LB) film transfer the wafers were immersed vertically into the water subphase before the film was prepared at the interface. The barriers were compressed to the designated surface pressure Π and the films were transferred onto the substrate by pulling the substrate out of the subphase at a transfer speed of 0.1 mm/min while the surface pressure was kept constant. For film transfer via surface lowering [27] hydrophilic silicon wafers were immersed into the subphase before spreading the dU11 at the

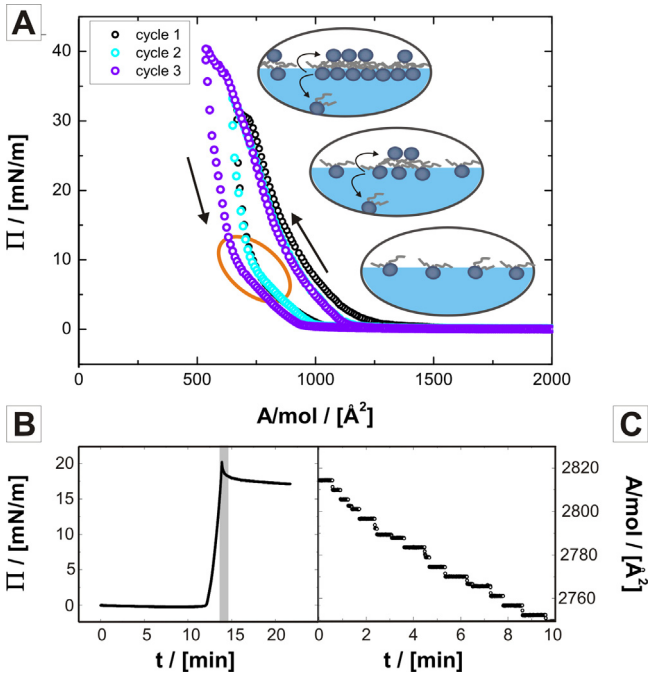

Fig. 2. (A) Pressure–molecular area isotherms of one dU11 monolayer showing the first (black), second (turquoise) and third (purple) compression–expansion cycle. Arrows indicate direction of the barrier movement. Changes in curvature are indicated by an oval in the isotherm. The schemes outline possible structures formed at the air/water interface at increasing pressure (from bottom to top). (B) Surface pressure decrease of a dU11 film at the air/water interface at constant surface area $A = 14.4\,cm^2$. The gray bar marks the first minute after stopping the barriers. (C) Decrease of area per molecule of a dU11 film at the air/water interface at constant surface pressure $\Pi = 0.2$ mN/m. (For interpretation of the references to color in this figure legend, the reader is referred to the web version of the article.)

interface. The sample was hydrophilized as explained before and placed on a custom-made sample holder at an inclination of 6° relative to the air/water interface. Then, the dU11 solution was spread, left for solvent evaporation and compressed up to the designated surface pressure. The barriers were stopped and the subphase was pumped out of the Langmuir trough with a peristaltic pump at a pump rate of approximately 10 mL/min, thereby lowering the interfacial film onto the wafer. Calculations of the transfer ratios resulted in values > 1, independent of the actual quality of the transferred films. This is, because the transfer ratio in this special case of an instable system at the air/water interface is not a measure for the quality of the transferred film. Even the initial compression of the film results in a restructuring of the molecules in the film at the air/water interface.

2.4. Scanning force microscopy (SFM) measurements

The transferred films were investigated using a scanning force microscope (Veeco Dimension 3100, Veeco Digital Instruments, United States) in tapping mode equipped with silicon cantilevers (Olympus OMCL AC 240TS, nominal tip radius < 10 nm, resonance frequency: 50–90 kHz, spring constant: 0.7–3.8 N/m), which were coated with aluminum on the back side. Prior to the SFM measurements, the cantilevers were cleaned by placing them on a glass cover slip with the tip side facing an Ar-plasma for 30 s at a pressure of 1.6 mbar. SFM images were flattened and analyzed using Gwyddion Software (www.gwyddion.net). The surface coverage was determined by masking the covered regions and counting the according pixels in the SFM topography image using Gwyddion software. The ratio of the number of pixels displaying the covered area divided by the total number of pixels in the image was taken to be the surface coverage.

3. Results and discussion

3.1. Film stability at the interface

In order to investigate the stability of the dU11 molecules at the air/water interface Π–A isotherms were recorded as compression–expansion cycles (Fig. 2). The isotherms showed a continuous increase of the surface pressure upon compression at $A < 1390\,Å^2$. The onset of all compression–expansion cycles is defined as the area per molecule which corresponds to a surface pressure $\Pi = 0.5$ mN/m. A weakly pronounced kink at $\Pi = 7$ mN/m was observed upon expansion (marked by an oval in Fig. 2). Furthermore, no phase transitions or plateaus were found. Such isotherms indicate liquid like phase behavior and were also measured for the lipid dilauroylphosphatidylcholine (DLPC), which exhibits the same alkyl chain length as dU11 [28]. However, upon measuring Π–A isotherms, the DLPC molecules were found to start interacting with each other at an area per molecule of $120\,Å^2$ while the dU11 molecules start to interact at a much larger area per molecule of $1390\,Å^2$. The reason for this difference is attributed to the higher spatial occupancy of the oligonucleotide head group (M_W(dU11-headgroup) = 3289 g/mol) [24] compared to that of phosphatidylcholine group (M_W(PC) = 239 g/mol) assuming that the single stranded oligonucleotide behaves like a random coil.

We found that all isotherms exhibited a strong hysteresis between surface pressures measured during compression and expansion. Upon compression the surface pressure started increasing at an area per molecule of $1390\,Å^2$. Upon expansion the surface pressure was always lower compared to the compression at the same area and reached a surface pressure of $\Pi = 0.5$ mN/m at an area per molecule of $1040\,Å^2$. When increasing the maximum surface pressure from 31 - 33 mN/m in cycle 1 and 2 to 40 mN/m in cycle 3 this hysteresis became more pronounced: the expansion regime was shifted by $68\,Å^2$ for cycle 3 with respect to the expansion regime of cycle 1 and 2 at a $\Pi = 10$ mN/m. In addition, it is noteworthy that the expansion regime of cycle 2 was widely congruent with the expansion regime of the cycle 1 and the compression of the cycle 3 was widely congruent with the compression of cycle 2. However the compression regimes of cycle 2 and 3 were shifted from $1390\,Å^2$ to $1200\,Å^2$ to $1160\,Å^2$ at $\Pi = 0.5$ mN/m with respect to cycle 1.

As phospholipids [29] and other surfactants [30] containing a double hydrocarbon chain behaved in a similar way, we attribute this memory effect to an aggregation of the hydrophobic moieties of neighboring dU11 molecules at the air/water interface, despite the voluminous oligonucleotide head group. Rodríguez Patino et al. reported for dipalmitoylphosphatidylcholine (DPPC) that the memory effect was more pronounced after the first isotherm than for the successive ones [31], similar to our observation. The main difference between both systems is that we observed them before reaching the film collapse, while Rodríguez Patino et al. observed them mainly after collapse of their system. They attributed this effect to changes in monolayer morphology at the microscopic level due to self-association of the DPPC molecules after the first compression of the monolayer. Both effects, hysteresis and isotherm shifts, have been observed by Niño et al. [32] for dioleoylphosphatidylcholine (DOPC) at surface pressures close to the collapse pressure. Niño et al. attributed both effects to relaxation phenomena inside the film at the air/water interface. Unlike Niño et al. [32] we have observed the existence of hysteresis and shifts in the isotherms even before a clear signal of the collapse pressure was reached. We take this together with the fact that no

clear collapse pressure could be reached as an indication, that the dU11 monolayer as such is not fully stable at the air/water interface. Either the molecules dissolve in the subphase or undergo a reorganization at the air/water interface into a multilayer structure as sketched in Fig. 2A. To further investigate the stability of the dU11 molecules at the air/water interface we performed three more experiments:

(i) A dU11 film was compressed up to a surface pressure $\Pi = 20$ mN/m. Then the molecular area was kept constant by stopping the barriers (Fig. 2B). We measured a pressure decrease of 10% within the first minute after stopping the barriers. The decrease after 5 min corresponded to 14%. Upon stopping the barriers at a higher surface pressure of 40 mN/m, we measured an area per molecule decrease of 20% after 1 min (Supporting Information Fig. S3). Thus a higher surface pressure resulted in a more pronounced surface pressure drop.

(ii) A dU11 film was compressed to a surface pressure of $\Pi = 0.2$ mN/m. Then the pressure was held constant by adjusting the area per molecule with the barriers (Fig. 2C). In this experiment the area per molecule decreased by 3% over a period of 10 min. Petrov et al. [33] reported a similar behavior for docosyl ethyl ether molecular layers at the air/water interface applying a constant surface pressure of 25 mN/m. In their experiments a decrease in area per molecule of 17% was observed over a time period of 10 min. Petrov et al. found that the decrease in surface pressure corresponded to the formation of multilayers at the air/water interface even before the collapse pressure was reached, which was proven on the Langmuir trough by Brewster angle microscopy imaging [33]. In analogy, it is also possible for the dU11 molecules to form multilayers at the air/water interface, even at low surface pressures, which again confirms that the dU11 molecules form very instable films at the air/water interface.

(iii) In our experiments we could never exceed a maximum surface pressure of $\Pi = 40$ mN/m irrespective of the amount of molecules spread onto the air/water interface. Furthermore we did not observe a clear maximum pressure upon which the dU11 molecular layers collapse. Therefore a certain collapse pressure could not be defined from the isotherms [34]. Thus, a successive collapse of the molecular layers upon compression and the formation of multilayers at the air/water interface are likely.

We conclude from isotherm measurements that the dU11 interfacial films were semi-stable. Relaxation of the interfacial films was realized by two processes: the dissolution of molecules from the air/water interface and the formation of multilayers at the air/water interface. From the results so far it was unclear, which of the effects is dominant. Therefore we performed SFM measurements of films transferred onto solid substrates.

3.2. Film transfer

Transferring a dU11 film from the air/water interface onto a silicon substrate via LB film transfer was possible at a slow transfer rate of 0.1 mm/min. SFM imaging of a dU11 film, which was transferred at a surface pressure of $\Pi = 5$ mN/m revealed that the sample changed with the number of scans (Fig. 3A and B). In the first scan (Fig. 3A) the substrate (0) and two different dU11 layers (1 and 2) with different heights were visible. Both layers were flat and homogeneous. No aggregates were visible. The first layer (layer 1) was 1.6 ± 0.1 nm thick, while the second and upper layer (layer 2) was 3.5 ± 0.1 nm thick with respect to the substrate (area 0). Thicknesses were determined by fitting the median height difference between substrate and film via a profile using Gwyddion Software (Fig. 3D). In addition, the simultaneously recorded phase contrast image exhibited a distinguishable phase contrast between each layer (Fig. 3C).

In order to interpret the SFM data we determined the sizes of the dU11 components roughly: the radius of gyration R_g (11mer) of a single stranded oligonucleotide 11mer is estimated to be R_g (11mer) = 0.8 nm in water [35]. The alkyl chains are not rigid. Therefore, they probably lie flat on top of the more voluminous single stranded oligonucleotide coil when deposited on a flat substrate (Supporting Information Fig. S4). The estimated length of one stretched alkyl chain is $l = 1.6$ nm, allowing an interaction between alkyl chains of neighboring dU11 molecules even if not fully stretched. The diameter of the alkyl chain corresponds to $d_{\text{alkyl}} = 0.4$ nm [36]. In this case ≈ 2 nm ($2 * R_g + d_{\text{alkyl}}$) thick wet films are expected. However, the films investigated with SFM were dry. During the drying process strong capillary forces tend to press the film onto the substrate which may reduce the film thickness to 1.6 nm, as determined by SFM measurements. In addition, the first layer was determined to be half as thick as the second one, indicating that the second, thicker layer actually consisted of two stacked monolayers, each being approximately 1.6 nm thick. We assume that the dU11 molecules inside layer 1 are oriented with the hydrophilic oligonucleotide moiety facing the hydrophilic substrate, while the hydrophobic alkyl chains face air. This is the typical orientation when transferring an amphiphilic monolayer onto a hydrophilic substrate via LB technique. Molecules in layer 2 would then arrange inversely with the alkyl chains facing layer 1 and the oligonucleotide moiety facing air. Comparison of height and phase image (Fig. 3A and C) shows that layers 1 and 2 exhibited a significant difference in the measured phase contrast. This indicates that both layers exhibited different interactions with the SFM tip and therefore the exposure of different interfaces to the tip [37]. For our system this is only possible when the hydrophilic or hydrophobic moieties of the dU11 molecule are exposed to the SFM tip, respectively. In particular, for layer 2 we obtain oligonucleotide exposed to the air interface, which covers about 32% in Fig. 3A. As briefly mentioned above, we found that by scanning with the SFM tip parts of the film were removed (Fig. 3A and B, blue oval). Material was removed from individual layers exposing the layer underneath which then resulted in a different phase contrast. Further SFM measurements at larger scan sizes at the same position did not reveal any material that was deposited at the edges of previous scans. Thus material was accumulated by the SFM tip, allowing for an inverse dip-pen nanolithography on the sample [38]. A similar effect has been observed for polyelectrolyte monolayers on mica, which were investigated with a surface force apparatus [39].

Furthermore, we investigated the structure of a film transferred at a higher surface pressure of $\Pi = 30$ mN/m (Fig. 4). In the topography image (Fig. 4A) again different layers (labeled with numbers 0, 1, 2, 3) were found. The film, which has been labeled as layer 1, covered most part of the substrate. A hole in the film exposed area 0 underneath corresponding to the substrate (Fig. 4B). Layer 1 is 2.6 ± 0.2 nm thick (Fig. 4C, dotted line) which is a little bit smaller than the value for a dU11 bilayer as derived from films transferred at lower pressures (3.5 ± 0.1 nm, Fig. 3) [40,41]. There are a second and third layer visible in the upper left corner of the topography image (Fig. 4A). The thickness of layer 2 with respect to the first bilayer is 3.8 ± 0.2 nm. The thickness of layer 3 with respect to the layer 2 is 4.0 ± 0.1 nm. Both values are close to the estimated thickness of one dU11 bilayer. Furthermore the phase contrast image supports the bilayer interpretation as we did not observe a significant phase contrast between layers 1, 2 and 3, which means that all three layers expose the same dU11 moiety to the SFM tip. From this we conclude that we image heights of three individual dU11 bilayers stacked on top of each other.

Then the film formation was investigated on a larger scale in dependence of the applied surface pressure from $\Pi = 2$ mN/m to

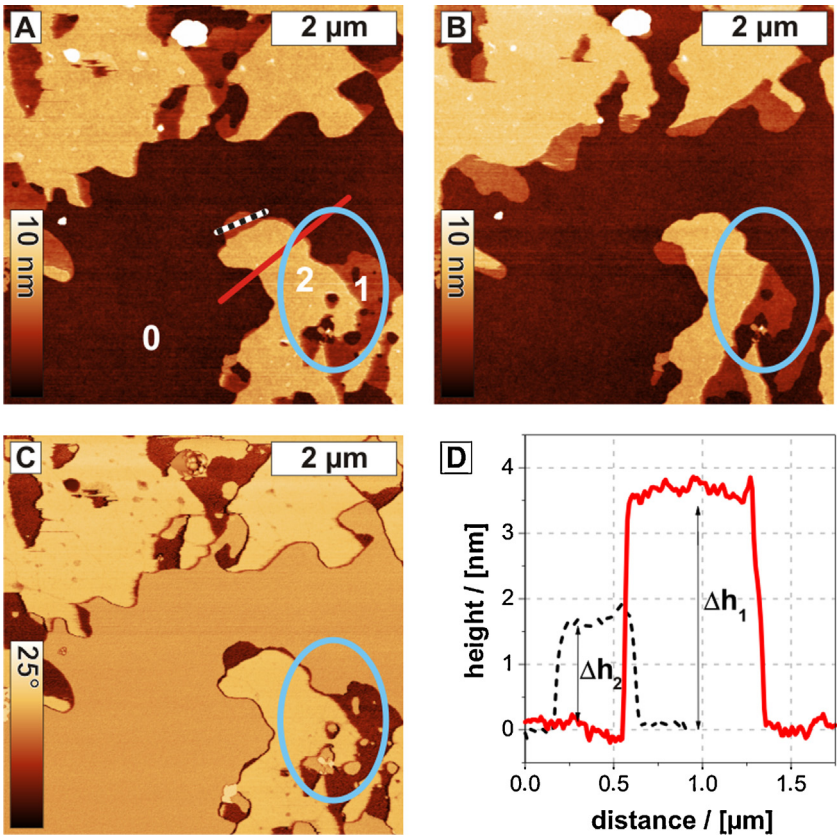

Fig. 3. SFM images of an LB film transferred at $\Pi = 5$ mN/m. (A) Height image of the first scan showing the substrate and a film with two different layers (1 and 2). Red and dashed lines mark the position of the line plots displayed in (D). (B) Height image of the second scan at the same position. Ovals mark the same region after the first and second scan. The topography between both scans changed, showing that the tip removed material from the sample when scanning. (C) Phase contrast image corresponding to (A). (D) Line plots mediated over 10 pixels at the positions marked in A to compare the thickness of layers 1 and 2. (For interpretation of the references to color in this figure legend, the reader is referred to the web version of the article.)

$\Pi = 30$ mN/m (Supporting Information Fig. S5). At a low surface pressure of $\Pi = 2$ mN/m the dU11 molecules formed a network. Additionally, the beginning of the formation of a more compact film is visible in the marked area (Supporting Information Fig. S5A, blue oval). Upon increasing the surface pressure to $\Pi = 5$ mN/m a film with a coverage of approximately 77% formed (Supporting Information Fig. S5B). A further surface pressure increase to $\Pi = 10$ mN/m lead to an increase of the surface coverage to 90% (Supporting Information Fig. S5D). At a surface pressure of $\Pi = 30$ mN/m we found a surface coverage of 95% (Supporting Information Fig. S5E). The average film thickness of all films shown in Supporting Information Fig. S5 was 3.2 ± 0.2 nm, which matches the thickness estimated for a dU11 bilayer. Accordingly, the oligonucleotide moieties of the dU11 molecules were facing the air interface. In conclusion this series of experiments showed that the dU11 molecule starts to form a bilayer film at a surface pressure of $\Pi = 2$ mN/m, the formation of multiple bilayers can be found at $\Pi \geq 30$ mN/m and the surface coverage increases upon increasing the surface pressure (Supporting Information Fig. S5C). Films transferred from a subphase containing salt showed a similar behavior (Supporting Information Fig.S9).

Taking into account all experiments, the first dU11 layer aligns with the hydrophilic oligonucleotide head facing the hydrophilic substrate (Fig. 5). The molecules in layer 2 are aligned inversely. Upon imaging each of the layers individually, a phase contrast can

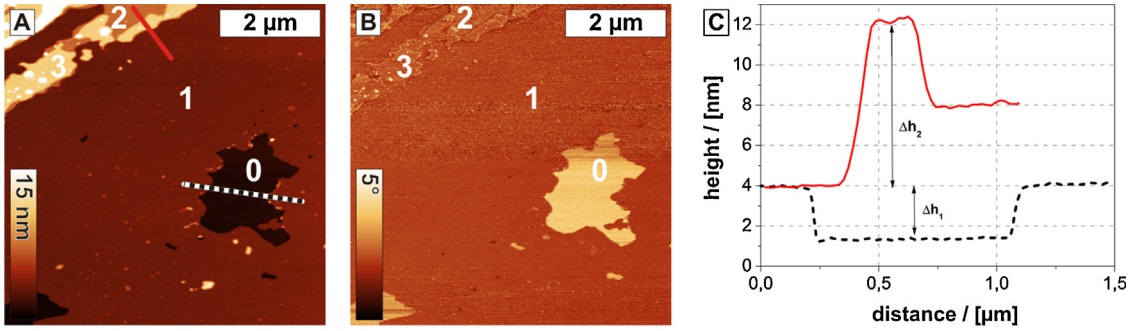

Fig. 4. SFM images of a LB-film transferred at $\Pi = 30$ mN/m. (A) Topography image showing the substrate and covered by a multilayered film. Red and dashed lines mark the position of the line plots displayed in (C). (B) Corresponding phase image showing a phase contrast between substrate and layer 1 of the film, but not between layers 1 and 2. (C) Line plots at the positions marked in image A mediated over 10 pixels. (For interpretation of the references to color in this figure legend, the reader is referred to the web version of the article.)

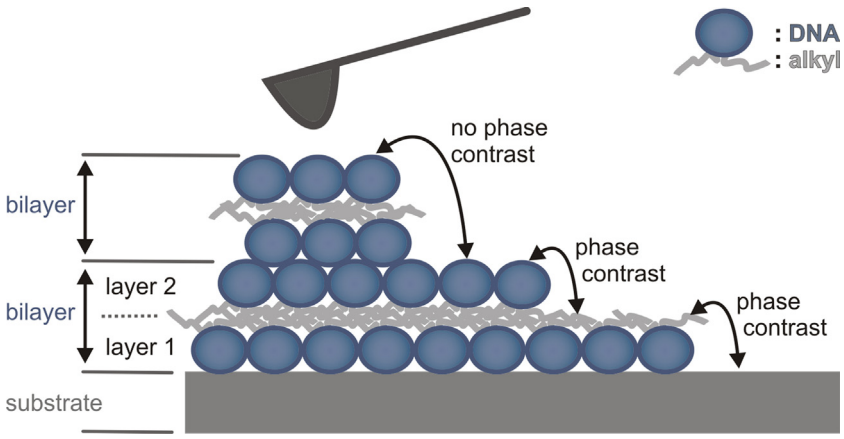

Fig. 5. Model proposed for the bilayer formation on the substrate and the according phase contrast in SFM phase images. The phase contrast between a dU11 mono- and bilayer is caused by the altered orientation of the molecules. The hydrophobic tails of the molecules are facing air in the first monolayer, the molecules in the second layer are oriented oppositely.

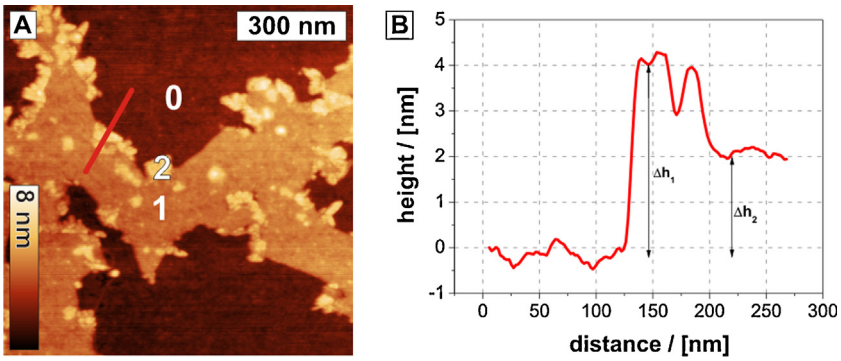

Fig. 6. (A) SFM height image of a dU11 film transferred via surface lowering at a surface pressure of $\Pi = 3$ mN/m. The red line marks the position of the line plot displayed in (B). (B) Line plot mediated over 10 pixels at the positions marked in (A) to compare the thickness of layers 1 and 2. (For interpretation of the references to color in this figure legend, the reader is referred to the web version of the article.)

be found between these layers. Then the origin of the phase contrast is the varying interaction between tip and hydrophilic or hydrophobic moiety of the dU11 molecule, respectively. Additionally, layers 1 and 2 are equally thick in the SFM height image. Stacking of a second bilayer on top of the first one (layer 1 + layer 2) leads only to a change in the measured height but not in the SFM phase contrast.

Furthermore, dU11 films were also transferred via surface lowering technique to investigate the influence of the transfer technique onto the morphology of the dU11 film. Here the aim was to exclude that the multilayer formation is a byproduct of the transfer technique. Films transferred via surface lowering at surface pressures of $\Pi = 3$ mN/m and $\Pi = 5$ mN/m both exhibited dU11 mono- and bilayers (Fig. 6). Layer 1 is 1.9 nm thick while layer 2 is twice as thick with 4 nm height. Therefore we have confirmed that the multilayer formation is not significantly influenced by the transfer technique probably.

Finally, we studied films of ssODN-*b*-PPO (as a second type of amphiphilic macromolecule containing an oligonucleotide sequence) transferred by the Langmuir Blodgett method. These molecules are characterized by an increase in molecular weight of the hydrophobic moiety while length of the oligonucleotide moiety remained constant (R_g (11mer) = 0.8 nm [35]). The radius

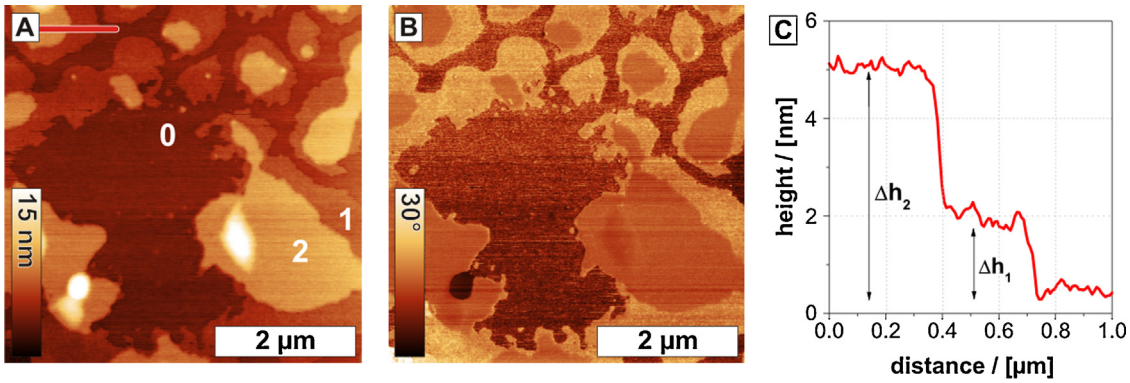

Fig. 7. SFM images of ODN-*b*-PPO ($M_W = 6800$ g/mol) films transferred onto hydrophilic solid substrates via LB film transfer. (A) SFM topography image of a ODN-*b*-PPO film transferred at a surface pressure of 30 mN/m. The red line marks the positions of the line plot in (C). (B) SFM phase image. (C) Line plot at the positions marked in image (A) mediated over 10 pixels. (For interpretation of the references to color in this figure legend, the reader is referred to the web version of the article.)

of gyration of the PPO polymer R_g (PPO) was estimated to be R_g (PPO) = 2.0 nm [42]. When transferred onto a substrate this yields a theoretical film thickness of 5.6 nm ($2 * R_g(11mer + 2 * R_g(PPO))$. The films transferred at a pressure of 30 mN/m showed also a SFM phase and height contrast (Fig. 7). Again, we identified the substrate (area 0) and two layers, layer 1 and 2, which exhibited a phase contrast difference. We estimated a thicknesses of layer 1 to be $\Delta h_1 = 1.8 \pm 0.2$ nm and layer 2 to be $\Delta h_2 = 5.0 \pm 0.3$ nm. In this case layer 1 probably corresponds to ODN-*b*-PPO molecules lying flat on the substrate, while layer 2 corresponds to molecules arranged perpendicular or at an angle to the substrate.

4. Conclusions

The dU11 molecules form semi-stable films at the air/water interface: Upon film compression the molecules exhibit relaxation phenomena like dissolution of dU11 molecules into the subphase but also reorganization into multiple layers at the air/water interface. SFM investigation of interfacial films transferred via Langmuir–Blodgett and surface lowering technique elucidated, that the formation of multiple layers at the air/water interface is one of the major relaxation mechanisms for films made from dU11 molecules. Presumably, the rearrangement of the molecules into bi- and multiple bilayers happens already at the air/water interface and is one of the reasons for the measured semi-stability of the dU11 films. The multilayer formation enables us to fabricate hydrophilic samples covered with dU11 molecules exposing at maximum 95% of ssODN to the air interface which might then be accessible for further recognition events like the target binding of aptamers or Watson–Crick base-pairing. Upon SFM imaging single dU11 layers can be removed individually in an analogous manner of inverse dip-pen nanolithography. This can enable patterning of oligonucleotide amphiphile films into desired regions of oligonucleotide or alkyl chains facing towards the air. The combination of multilayer formation at the interface on one hand opens the possibility to engineer the surface by inverse dip-pen lithography and, on the other hand, paves a new way for the preparation of functional thin films with tunable local organization of the individual layers with sequence defined molecular recognition ability.

Acknowledgements

We acknowledge partial financial support from DFG (SFB 625 From Single Molecules to Nanoscopically Structured Materials). Furthermore we acknowledge Hans Riegler, Uwe Rietzler and Karlheinz Graf for support and discussions while perfroming experiments.

Appendix A. Supplementary data

Supplementary data associated with this article can be found, in the online version, at http://dx.doi.org/10.1016/j.colsurfb.2013.06.022.

References

[1] C.M. Niemeyer, Curr. Opin. Chem. Biol. 4 (2000) 609–618.
[2] H. Liu, D. Liu, Chem. Commun. (2009) 2625–2636.
[3] J. Bath, A.J. Turberfield, Nat. Nanotechnol. 2 (2007) 275–284.
[4] B. Yurke, A. Turberfield, A. Mills, F. Simmel, J. Neumann, Nature 406 (2000) 605–608.
[5] Z. Li, Y. Zhang, P. Fullhart, C.A. Mirkin, Nano Lett. 4 (2004) 1055–1058.
[6] M. Kwak, A. Herrmann, Angew. Chem. Int. Ed. 49 (2010) 8574–8587.
[7] A. Patwa, A. Gissot, I. Bestel, P. Barthélémy, Chem. Soc. Rev. 40 (2011) 5844–5854.
[8] M. Kwak, A. Herrmann, Chem. Soc. Rev. 40 (2011) 5745–5755.
[9] M.P. Thompson, M.-P. Chien, T.-H. Ku, A.M. Rush, N.C. Gianneschi, Nano Lett. 10 (2010) 2690–2693.
[10] N. Cottenye, M.-I. Syga, S. Nosov, A.H.E. Mueller, L. Ploux, C. Vebert-Nardin, Chem. Commun. 48 (2012) 2615–2617.
[11] K. Ding, F.E. Alemdaroglu, M. Börsch, R. Berger, A. Herrmann, Angew. Chem. Int. Ed. 46 (2007) 1172–1175.
[12] A. Kurz, A. Bunge, A.-K. Windeck, M. Rost, W. Flasche, A. Arbuzova, et al., Angew. Chem. Int. Ed. 45 (2006) 4440–4444.
[13] M. Hadorn, P.E. Hotz, PLoS ONE 5 (2010).
[14] P.A. Beales, J. Nam, T.K. Vanderlick, Soft Matter 7 (2011) 1747–1755.
[15] Y.-H.M. Chan, B. van Lengerich, S.G. Boxer, Proc. Natl. Acad. Sci. U. S. A. 106 (2009) 979–984.
[16] G. Stengel, R. Zahn, F. Hook, J. Am. Chem. Soc. 129 (2007) 9584.
[17] B. Städler, D. Falconnet, I. Pfeiffer, F. Höök, J. Vörös, Langmuir 20 (2004) 11348–11354.
[18] H. Kitano, H. Ringsdorf, Bull. Chem. Soc. Jpn. 58 (1985) 2826–2828.
[19] E.A. Montanha, F.J. Pavinatto, L. Caseli, O. Kaczmarek, J. Liebscher, D. Huster, et al., Colloids Surf. B 77 (2010) 161–165.
[20] E. Montanha, L. Caseli, O. Kaczmarek, J. Liebscher, D. Huster, O.N. Oliveira Jr., Biophys. Chem. 153 (2011) 154–158.
[21] L. Caseli, C.P. Pascholati, F. Teixeira Jr., S. Nosov, C. Vebert, A.H.E. Müeller, et al., J. Colloid Interface Sci. 347 (2010) 56–61.
[22] M. Anaya, M. Kwak, A.J. Musser, K. Müllen, A. Herrmann, Chem. Eur. J. 16 (2010) 12852–12859.
[23] M. Anaya, PhD, 2010.
[24] M. Kwak, I.J. Minten, D.-M. Anaya, A.J. Musser, M. Brasch, R.J.M. Nolte, et al., J. Am. Chem. Soc. 132 (2010) 7834–7835.
[25] F.E. Alemdaroglu, K. Ding, R. Berger, A. Herrmann, Angew. Chem. Int. Ed. 45 (2006) 4206–4210.
[26] K.B. Blodgett, J. Am. Chem. Soc. 56 (1934) 495.
[27] N. Vogel, L. De Viguerie, U. Jonas, C.K. Weiss, K. Landfester, Nicolas, et al., Adv. Funct. Mater. 21 (2011) 3064–3073.
[28] T. Oguchi, K. Sakai, H. Sakai, M. Abe, Colloids Surf. B 79 (2010) 205–209.
[29] J. Miñones, J.M. Rodríguez Patino, O. Conde, C. Carrera, R. Seoane, Colloids Surf. A 203 (2002) 273–286.
[30] A.M. Gonçalves da Silva, R.S. Romão, A. Lucero Caro, J.M. Rodríguez Patino, J. Colloid Interface Sci. 270 (2004) 417–425.
[31] J. Rodríguez Patino, A. Caro, M. Rodriguez Niño, A. Mackie, A. Gunning, V. Morris, Food Chem. 102 (2007) 532–541.
[32] M. Niño, A. Lucero, J. Patino, Colloids Surf. A 320 (2008) 260–270.
[33] J.G. Petrov, T.D. Andreeva, H. Möhwald, Langmuir 22 (2006) 4136–4143.
[34] C. Gicquaud, J.-P. Chauvet, G. Grenier, P. Tancrède, G. Coulombe, Biopolymers 70 (2003) 289–296.
[35] J. Zhou, S.K. Gregurick, S. Krueger, F.P. Schwarz, Biophys. J. 90 (2006) 544–551, http://dx.doi.org/10.1529/biophysj.105.071290.
[36] G. Nelles, H. Schönherr, M. Jaschke, H. Wolf, M. Schaub, J. Küther, et al., Langmuir 14 (1998) 808–815.
[37] R. García, R. Pérez, Surf. Sci. Rep. 47 (2002) 197–301.
[38] Y. Zhang, R. Berger, H.-J. Butt, in: B. Bushan (Ed.), Encyclopedia of Nanotechnology, Springer, 2012.
[39] K. Lowack, C.A. Helm, Macromolecules 28 (1995) 2912–2921.
[40] S. Vannoort, K. Vanderwerf, B. Degrooth, N. Vanhulst, J. Greve, Ultramicroscopy 69 (1997) 117–127.
[41] Y. Ebenstein, E. Nahum, U. Banin, Nano Lett. 2 (2002) 945–950.
[42] K. Mortensen, J. Phys.: Condens. Matter 8 (1996) A103–A124.